

Spatial change detection using voxel classification by normal distributions transform

Ukyo Katsura¹, Kohei Matsumoto¹, Akihiro Kawamura², Tomohide Ishigami³,
Tsukasa Okada³, and Ryo Kurazume²

Abstract—Detection of spatial change around a robot is indispensable in several robotic applications, such as search and rescue, security, and surveillance. The present paper proposes a fast spatial change detection technique for a mobile robot using an on-board RGB-D/stereo camera and a highly precise 3D map created by a 3D laser scanner. This technique first converts point clouds in a map and measured data to grid data (ND voxels) using normal distributions transform and classifies the ND voxels into three categories. The voxels in the map and the measured data are then compared according to the category and features of the ND voxels. Overlapping and voting techniques are also introduced in order to detect the spatial changes more robustly. We conducted experiments using a mobile robot equipped with real-time range sensors to confirm the performance of the proposed real-time localization and spatial change detection techniques in indoor and outdoor environments.

I. INTRODUCTION

Spatial change detection is a fundamental technique for finding the differences between two or more pieces of geometrical information. This technique is critical in several applications, such as topographic change detection in airborne laser scanning [1] [2] or terrestrial laser scanning [3] [4], map maintenance in urban areas [5], preservation of cultural heritage [6], and analysis of plant growth [7]. In robotics, detection of spatial changes around a robot is indispensable in several robotic applications, such as search and rescue, security, and surveillance. Service robots, such as cleaning robots or delivery robots, which are used on a daily basis, require the ability of spatial change detection in order to safely and efficiently co-exist with humans, because the environment can change dynamically according to human behavior. For these service robots, precise localization is also required in order to perform a desired task.

Two-dimensional LiDARs, such as Hokuyo TOPURG and Sick TiM51x, have commonly been used for the localization of mobile robots due to their low cost, small size, and high precision [8][9][10]. On the other hand, in recent years, with the widespread use of low-cost 3D laser scanners, such as FARO Focus 3D, and 3D range sensors, such

as Kinect, Xtion, and Velodyne HDL-32e, 3D localization (or 6D localization, including attitude) is also becoming available in robotic applications using highly accurate 3D mapping and real-time 3D range data. However, in general, data measured by these sensors consist of millions of 3D points, which are referred to collectively as a point cloud. Real-time processing of a large number of point clouds is therefore not a trivial task. For example, although iterative closest point (ICP) [11] is a popular technique for aligning point clouds, ICP requires the determination of point-to-point (or mesh) correspondences, and thus the calculation cost remains too large for real-time localization or spatial change detection by a mobile robot using point clouds.

In order to deal with the enormous number of points in a point cloud for robust robot localization, we have proposed a fast localization technique using normal distributions transform (NDT)[12] and a particle filter [13]. In the present paper, as an additional function of the proposed localization technique [13], we propose a fast spatial change detection technique by comparing 3D range data obtained by an on-board RGB-D/stereo camera and a high-precision 3D map created by a 3D laser scanner. This technique first converts point clouds in the map and measured data to grid data (ND voxels) by NDT, and classifies the voxels into three categories. The voxels in the map and the measured data are then compared according to the category and features of ND voxels. Overlapping and voting techniques are also introduced in order to detect spatial changes more robustly. We conducted the experiments using a mobile robot equipped with real-time range sensors in order to confirm the performance of the proposed real-time localization and spatial change detection techniques in indoor and outdoor environments.

II. RELATED RESEARCH

Spatial change detection is a critical problem in some robotic applications [14] [15] [16] [17] [18], [19]. Andreasson et al. [14] proposed autonomous change detection for a security patrol robot. They used color and depth information obtained from a 3D laser range finder and a camera. A precise reference model was first created from multiple color and depth images and was registered by 3D normal distributions transform (3D-NDT) [20] representation. Spatial changes are detected by calculating the probabilistic value of the current point being different from the reference model using the 3D-NDT representation and color information. Saarinen et al. [21] proposed Normal Distributions Trans-

¹Ukyo Katsura and Kohei Matsumoto are with Graduate School of Information Science and Electrical Engineering, Kyushu University, Fukuoka 819-0395, Japan {katsura, matsumoto}@irvs.ait.kyushu-u.ac.jp

²Akihiro Kawamura and Ryo Kurazume are with Faculty of Information Science and Electrical Engineering, Kyushu University, Fukuoka 819-0395, Japan {kawamura, kurazume}@ait.kyushu-u.ac.jp

³Tomohide Ishigami and Tsukasa Okada are with Panasonic Inc., 3-1-1 Yagumo-naka-machi, Moriguchi City, Osaka 570-8501, Japan {ishigami.tomohide, okada.tsukasa}@jp.panasonic.com

form Occupancy Maps (NDT-OM), which concurrently represent the occupancy probability and the shape distribution of points (NDT) in each voxel. The occupancy probability is calculated from a sensor model and the point distribution in the voxel, and the similarity measure of two NDT-OMs is defined by L_2 distance function. Nùñez et al. [15] proposed a fast change detection technique using a mixture Gaussian model and a fast and robust matching algorithm. Point-based comparison of an environmental model and a large number of point cloud data measured by an on-board range sensor requires a large calculation cost. In order to solve this problem, they represented the environmental model and the measured data with a mixture Gaussian model and processed the difference calculation using a high-speed algorithm. Fehr et al. [18] presents a 3D reconstruction technique of dynamic scenes involving movable objects using the truncated signed distance function (TSDF). They represented the current scene with TSDF grids and compared them with previous TSDF grids to obtain segmented movable objects in the scene. Luft et al. [19] proposed a stochastic approach to evaluate whether a grid is changed in time according to full-map posteriors represented by real-valued variables. Their technique enables consideration of the full-path information of the laser measurement, as opposed to end-point based approaches. Moreover, it considers the confidence about the cell values as opposed to occupancy maps or a most-likely maps.

In general, spatial change detection can be classified into three groups: point/mesh-based, height-based, and voxel-based comparisons. Point/mesh-based comparison [22] [6] is a technique that compares the distance of nearest points or meshes in two point clouds, which is similar to the ICP algorithm [23]. Lague et al. [4] proposed the use of the distance along normal direction of a local surface to make the algorithm robust to errors in 3D terrain data measured by a terrestrial laser scanner. In [3], point clouds are converted to panoramic distance images, which are compared directly. The problem with this technique is the degree to which the proper threshold is determined [22].

Height-based comparison is often used in geographical analysis in earth sciences. The digital elevation map (DEM) of difference (DoD) is a popular technique to compare geographical data captured by airborne or terrestrial laser scanners [5] [24] [2]. This technique also has the problem of selecting a proper threshold.

In voxel-based comparison, a point cloud is first converted to a voxel representation using, for example, an octree structure. Performing the XOR of occupancy voxels is the simplest way [25] to find spatial differences. In [26], three metrics are compared in order to calculate the difference of voxels, which are the average distance, the plane orientation, and the Hausdorff distance. The Hausdorff distance is the maximum value of the minimum distances of points in two voxels and indicates the best performance. However, the computational cost of the Hausdorff distance is quite high, because closest point pairs must be determined. In spatial change detection in 3D, not only point clouds but also a

sequence of camera images has been used [27], [28].

The proposed technique is a voxel-based comparison method. However, rather than comparing the distances of points or meshes or the existence of occupied voxels directly, we used the point distribution in each voxel calculated by 3D-NDT. We classify the distribution of points in a voxel into three categories and compare the voxels in different scans according to the category of voxels. Although Andreasson et al. [14] also used 3D-NDT for spatial change detection, their technique can be classified as a point-based comparison because they used 3D-NDT to calculate the probability of a point being different from the reference model.

III. FAST 3D LOCALIZATION USING NDT AND A PARTICLE FILTER

We have proposed a fast 3D localization technique using a large-scale 3D environmental map measured by a 3D laser scanner and 3D range data captured by an RGB-D/stereo camera on a mobile robot [13].

The proposed technique uses the idea of NDT [11] for expressing a point distribution in a compact but information-rich form. Point clouds in an environmental map are first converted to the ND voxel representation. Then, in order to more efficiently handle the characteristics of point distribution, representative planes called eigenplanes are extracted and registered as a new environmental map representation. Next, when a mobile robot scans the surrounding environment using an on-board RGB-D/stereo camera, an obtained 3D point cloud is also converted to the ND voxel representation and eigenplanes are extracted in the same manner for the environmental map. In addition, seven representative points (six sigma points and a center point) are extracted and registered as additional features. Finally, the similarities between the environmental map and the measured data are examined based on plane-and-plane and point-and-plane correspondences. Using the obtained similarities, a particle filter is used to find the optimum position, which indicates the maximum similarity between the environmental map and the measured data.

IV. FAST SPATIAL CHANGE DETECTION USING ND VOXELS

In this section, we propose a fast spatial change detection technique using ND voxels, which are generated and used for the localization [13] mentioned in Section III. The most simple technique for spatial change detection using voxels is to compare the existence of occupied voxels in a same space by XOR operation [25], in which a spatial change is considered to have occurred if an occupied voxel exists on the map data but does not exist in the measured data, or vice versa. However, due to quantization errors or localization and measurement errors, this simple technique does not work well in many cases. For example, if the localization error is larger than the voxel size, most of the voxels are labeled as spatial changes. In order to tackle this problem and realize robust spatial change detection, the technique proposed in this section adopts the following three techniques.

- 1) Classification of point distribution in an ND voxel
- 2) Overlapping of voxels in map data
- 3) Voting of spatial change detection through sequential measurements

A. Classification of point distributions in ND voxels

If we use the simple technique for spatial change detection by taking XOR between the map and the measured voxels mentioned above, it is impossible to detect spatial changes if the voxel includes not only point clouds to be detected as spatial change but also other stationary point clouds such as a floor or a wall. The proposed technique solves this problem by classifying the point distribution in ND voxels into three categories.

In the calculation of NDT during the localization [13], three eigenvalues $\lambda_1, \lambda_2, \lambda_3$ ($\lambda_1 < \lambda_2 < \lambda_3$) and eigenvectors of a covariance matrix of a point cloud in a voxel are obtained. According to the following criteria, we classify the point distribution in ND voxels into three categories, that is, “Sphere”, “Sheet”, and “Line”. In addition, if there are no measured points in a voxel, then we refer to the voxel as “Empty”.

$$\textit{Sphere} \quad \lambda_3 \approx \lambda_2 \approx \lambda_1 \gg 0 \quad (1)$$

$$\textit{Sheet} \quad \lambda_3 \approx \lambda_2 \gg \lambda_1 \approx 0 \quad (2)$$

$$\textit{Line} \quad \lambda_3 \gg \lambda_2 \approx \lambda_1 \approx 0 \quad (3)$$

Magnusson et al. [29] also proposed a loop detection technique using the histogram of three shapes (spherical, planar, and linear), which are classified from point clouds according to the eigenvalues. In our case, we use these classifications to evaluate the difference between the map and measured voxels.

If the voxels in the map and measured data are labeled with different categories, then we say that there is a spatial change in this space of the voxel. In addition, even if both voxels have the same labels of “Sheet” or “Line”, we compare the normal or direction vectors of the sheets and the lines, which are the eigenvectors corresponding to minimum and maximum eigenvalues, respectively. If these vectors are sufficiently matched, then we consider these voxels to have the same labels and ignore their spatial change.

$$(\mathbf{n}_{map}, \mathbf{n}_{measured}) < N_t \quad (\textit{Sheets}) \quad (4)$$

$$(\mathbf{v}_{map}, \mathbf{v}_{measured}) < V_t \quad (\textit{Lines}) \quad (5)$$

where \mathbf{n} and \mathbf{v} are the normal and direction vectors of the sheets and the lines which are eigenvectors corresponding to the smallest and the largest eigenvalues, and N_t and V_t are proper thresholds. \mathbf{n}_{map} and \mathbf{v}_{map} are calculated beforehand from the environmental map (point cloud) measured by a 3D laser scanner, and $\mathbf{n}_{measured}$ and $\mathbf{v}_{measured}$ are obtained using the measured map (point cloud) by an on-board RGB-D/stereo camera. In the experiments in Section VI, we set N_t and V_t as 0.5. Similar idea can be seen in [26], in which “best fitting plane orientation” was used to evaluate the spatial changes.

B. Overlapping of voxels in map data

The proposed technique inherently involves a quantization error because we divide the entire space into several voxel grids and perform NDT for each voxel. Thus, the classification mentioned above is also affected by the quantization error. For example, the boundary between a floor and a wall is classified as “Sheet” if the majority of points in the voxel belong to either a floor or a wall. On the other hand, the boundary is classified as “Sphere” if both planes are evenly included.

In order to suppress the influence of quantization error, the proposed technique uses overlapping ND voxels [12]; that is, adjacent voxels overlap each other so that the centers of the voxels are displaced with half the voxel size. As a result, every point in 3D space is involved with eight adjacent voxels. Thus, by comparing a voxel in the measured data with up to 27 adjacent voxels in the map data, we can evaluate the degree of coincidence of the map and the measured data robustly with respect to the quantization error. More precisely, if at least one voxel in 27 voxels in the map data is similar enough to the voxel in the measured data, that voxel is marked as “no change”. In the proposed technique, the ND voxels in the map overlap, and ND voxels are calculated beforehand in order to reduce the on-line calculation cost.

C. Voting of spatial change detection through sequential measurements

The measurement data taken from an RGB-D/stereo camera, such as Kinect or a stereo camera, are corrupted by noise, and the measurement noise tends to be detected as spatial change in some cases. Therefore, we adopt a voting technique through sequential measurements in order to suppress the effect of the measurement noise. Here, we first extract the voxels that are regarded as spatially changed voxels in each measured datum. Then, by voting on these results for the space in a global coordinate system with the following weights according to the 3D normal distribution, the regions of spatial change can be obtained robustly.

$$w(\mathbf{p}) = N(\mathbf{c}, \sigma^2) \quad (6)$$

where \mathbf{p} is the center of the adjacent voxel in the map data and \mathbf{c} is the center of the original voxel in the measured data.

In the experiments in Section VI, we set the voxel size as 400 mm and σ as 200 mm, and voted for the information of the spatial change to 27 adjacent voxels.

V. MOBILE ROBOT SYSTEM FOR LOCALIZATION AND SPATIAL CHANGE DETECTION

In order to confirm the performance of the proposed localization and spatial change detection techniques, we built a mobile robot system equipped with an omni-directional laser scanner (Velodyne HDL-32e) and an RGB-D camera (Kinect for Xbox One, Microsoft), as shown in Fig. 1. For localization, point cloud data measured by the omni-directional laser scanner are compared with a large-scale 3D map measured by a high-precision laser scanner (Focus 3D,

FARO). However, the number of scanning lines of the omni-directional laser scanner is 32, which is not sufficient for detecting spatial changes in small regions. Thus, the RGB-D camera is used to capture detailed range data in front of the robot for spatial change detection.



Fig. 1. Mobile robot system equipped with an omni-directional laser scanner (Velodyne HDL-32e) and an RGB-D camera (Kinect, Microsoft).

VI. EXPERIMENTS IN INDOOR AND OUTDOOR ENVIRONMENTS

A. Indoor experiments

We conducted an experiment for spatial change detection in an indoor environment (a hall) in order to confirm the performance of the proposed technique. We first scanned the hall from eight positions using a high-precision laser scanner (Faro Focus 3D) and obtained an environmental map with dimensions of 40 m \times 11 m. Figure 2 shows the obtained 3D point cloud and ND voxel representation.

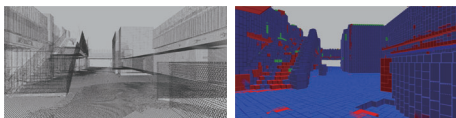


Fig. 2. 3D environmental map and ND voxel representation. Red, green, and blue cubes are voxels labeled sphere, line, and sheet, respectively.

Next, we placed three objects, as shown in Fig. 4, having dimensions of (a) 10 cm \times 10 cm \times 10 cm (① and ⑤), (b) 20 cm \times 20 cm \times 20 cm (② and ⑥), (c) 30 cm \times 30 cm \times 30 cm (③ and ⑦), and (d) 40 cm \times 40 cm \times 40 cm (④ and ⑧) at the positions shown in Fig. 3. The robot (Fig. 1) then moves along the trajectory shown in Fig. 3 and attempts to find these objects as spatial changes.

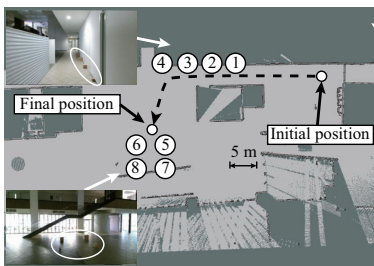


Fig. 3. Indoor environment (Hall: 40 m \times 11 m).

The initial position of the robot is determined as follows. An initial position is first roughly assigned by hand. The accurate position is then estimated using the omni-directional

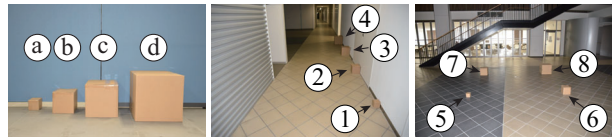


Fig. 4. Objects placed in the pathway.

laser scanner and the environmental map by the positioning technique in Section III [13], which is based on the comparison of ND voxels and optimization using a particle filter. The target position is determined manually, and the path to the target position is determined by Dijkstra's algorithm in the navigation package in the robot operating system (ROS). The robot moves along the desired path automatically and fuses the position information from the particle filter [13] and odometry at 1 Hz. The range data from the RGB-D camera (measured data) are transformed using the estimated position information and compared with the environmental map using the proposed technique. In this experiment, the voxel size for localization and the spatial change detection is 40 cm.

Table I shows the positioning errors in cases that the voxel size is 40 [cm] and 100 [cm]. The actual robot position is measured by the high-precision laser scanner (Faro Focus 3D) placed at a known position. In this experiment, the number of particles is fixed to 400. From this table, we can see that the accuracy for the localization is about 10 [cm] and not so different for the cases that the voxel sizes are 40 [cm] and 100 [cm].

TABLE I
POSITIONING ERRORS

Voxel size	Error
40 [cm]	99.2 [mm]
100 [cm]	104.6 [mm]

Figure 5(e) shows the detected spatial changes by the proposed method. Though one region is misdetecting as indicated by a white circle, the four kinds of objects that are placed at eight positions later are correctly detected in this experiment. We run the robot from the same initial position to the target position by taking RGB-D data ten times, and obtained the detection rate of the spatial changes as shown in Table II. Note that we considered the object is detected in case that at least one voxel containing vertexes, edges, or planes of the object is detected as spatially changed.

TABLE II
THE DETECTION RATE FOR FOUR KINDS OF OBJECTS

Object (size)	Detection rate [%]		
	Proposed	3D-NDT[14]	L_2 [21]
A (400 \times 400 mm)	100	100	95
B (300 \times 300 mm)	100	100	95
C (200 \times 200 mm)	85	75	50
D (100 \times 100 mm)	50	15	0

We also compared the performance of the proposed method with the 3D-NDT based spatial change detection

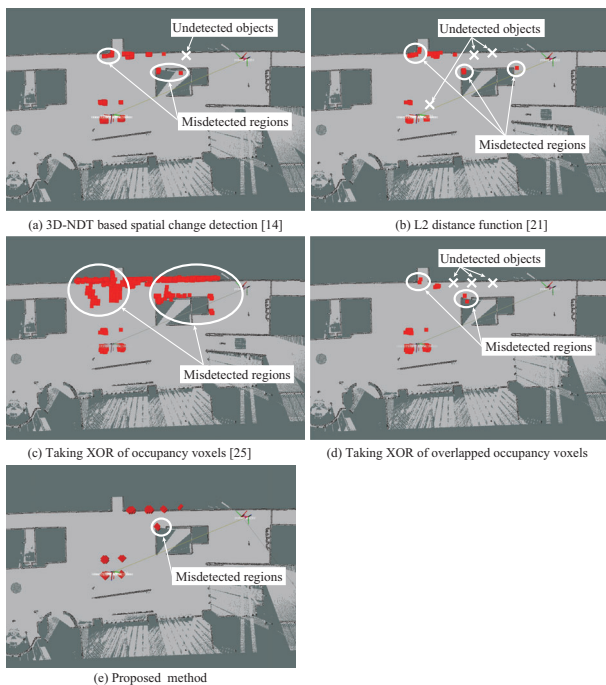


Fig. 5. Detected changes by (a) 3D-NDT based spatial change detection [14], (b) L_2 distance function [21], (c) taking XOR of occupancy voxels [25], (d) taking XOR of overlapped occupancy voxels, and (e) proposed method. Misdetected regions and undetected objects are indicated by white circles and crosses.

by Andreasson et al. [14], L_2 distance function [21], and simple methods using XOR calculation [25]. Figure 5(a) shows the detected spatial changes by the 3D-NDT based method [14]. In this experiment, we used the depth images captured by the RGB-D camera only and the color images were not used. Although the changed regions are mostly detected, some regions are misdetected or undetected. Table II shows the detection rate for each object by the 3D-NDT based spatial change detection after ten trials. These results show that the proposed method outperforms the 3D-NDT based spatial change detection especially in case that small objects are placed. Although it may be possible to improve the detection rate by decreasing the threshold for evaluating the spatial change, this induces many misdetection as shown in Fig. 5(a).

Figure 5(b) shows the detected spatial changes by L_2 distance function [21]. Figures 5(c) and (d) show the detected spatial changes by taking XOR between the map and the measured voxels [25]. Figure 5(d) uses the overlapped voxels in the map and we judged that the voxel is not spatially changed if at least one voxel among 27 map voxels adjacent to the measured voxel is occupied. In these experiments using XOR calculation, a number of misdetections are found, which are mainly caused by the positioning error of the mobile robot. On the other hand, the proposed method (Fig. 5(e)) is robust against position error due to voxel classification and voting technique.

Finally, we show the precision and recall of the detection of voxels which are specially changed for each method

in Table III. We used the overlapped voxels in the map and considered the voxel in the map should be detected as spatially changed if it contains vertexes, edges, or planes of the objects. Table III shows that the proposed method, which uses classification of point distribution, overlapping voxels, and voting techniques, gives highest precision (98.50 %) and outperforms other techniques. Figure 6 shows PR and ROC curves for each method using various parameters. In these figures, we can say that the proposed technique outperforms the conventional 3D-NDT [14] and L_2 distance based techniques. Note that the recalls are considerably low in all methods. This is because all voxels including at least one vertex, edge, or plane of the object are regarded as the correct voxels to be detected, and therefore, for example, the voxels on a wall hidden by the object are considered as missing voxels which are not correctly detected.

TABLE III
PRECISION AND RECALL [%]

	Precision	Recall
3D-NDT [14]	61.90	4.79
L_2 [21]	81.19	1.11
XOR [25]	17.55	3.95
XOR (overlapped)	69.99	1.71
Classification	22.74	2.47
Classification, overlapping	61.77	26.06
Classification, overlapping, voting (Proposed)	98.50	7.58

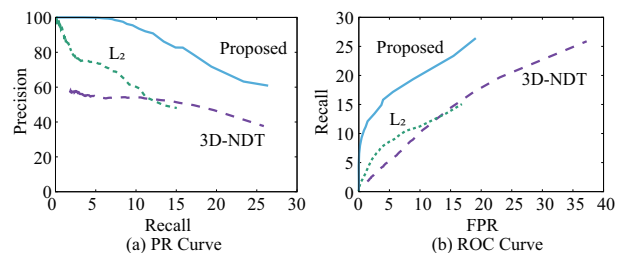


Fig. 6. PR and ROC curves.

B. Processing time for localization and spatial change detection

We measured the processing time for localization and spatial change detection in this experiment. Table IV shows the average processing time for one cycle of each step during the experiments (Intel Core i7, 3.40GHz). The average processing time for spatial change detection by the proposed technique is 21.3 millisecond including the conversion process of the depth images captured by the RGB-D camera to the ND voxel representation. On the other hand, the processing time by the 3D-NDT based spatial change detection [14] is 563.6 millisecond and the proposed technique is 26.5 times faster than the 3D-NDT based technique. The simple method using XOR calculation [25] is slightly faster than the proposed method. Note that, since these processes can be executed independently, we run processes of localization and spatial change detection at 1 Hz in the experiments.

TABLE IV
PROCESSING TIME FOR EACH STEP

Localization		827.2 [msec]
Spatial change detection	3D-NDT[14]	570.0 [msec]
	L_2 [21]	17.2 [msec]
	XOR[25]	17.9 [msec]
	XOR (overlapped)	19.4 [msec]
	Proposed	20.4 [msec]

C. Outdoor experiments

In these experiments, we first scan the outdoor environment (road) from three positions using a high-precision laser scanner (Faro Focus 3D) and obtained an environmental map having dimensions of 30 m \times 10 m. We then placed four objects having dimensions of ①, 40 cm \times 40 cm \times 40 cm; ②, 40 cm \times 40 cm \times 80 cm; ③, 80 cm \times 15 cm \times 60 cm; and ④, 40 cm \times 40 cm \times 20 cm, and the robot moves 30 m along a straight line. Here, we replaced the RGB-D camera with a conventional stereo camera system because acquiring range data in direct sunlight using the RGB-D camera (Kinect for Xbox One) becomes extremely difficult. We captured 430 range images using the stereo camera system during the movement.

Figure 8(a) shows the detected regions (red, green, and blue cubes), which are estimated to be spatially changed using XOR calculation of the occupied voxels [25]. Figures 8(b), 8(c), and 8(d) show the detected regions using the classification of point distribution (Section IV-A), classification and overlapping of voxels in map data (Section IV-B), and classification, overlapping, and voting of spatial change detection through sequential measurements (Section IV-C), respectively. In Fig. 8, detected voxels classified as ‘‘Sphere’’, ‘‘Sheet’’, and ‘‘Line’’ are illustrated by red, blue, and green cubes, respectively. Table V shows the number of voxels detected as spatial changes in these experiments. As shown Fig. 8(d), the voxels with spatial changes are detected correctly if we apply all of the techniques proposed in Section IV, that is, classification of point distribution, overlapping of voxels in map data, and voting of spatial change detection.

TABLE V
NUMBER OF VOXELS DETECTED AS SPATIAL CHANGES

XOR	704
Classification	364
Classification and overlapping	313
Classification, overlapping, and voting (Proposed)	48

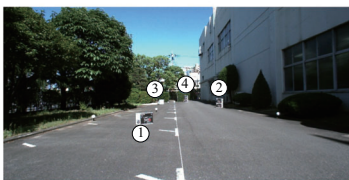


Fig. 7. Four additional objects in an outdoor environment.

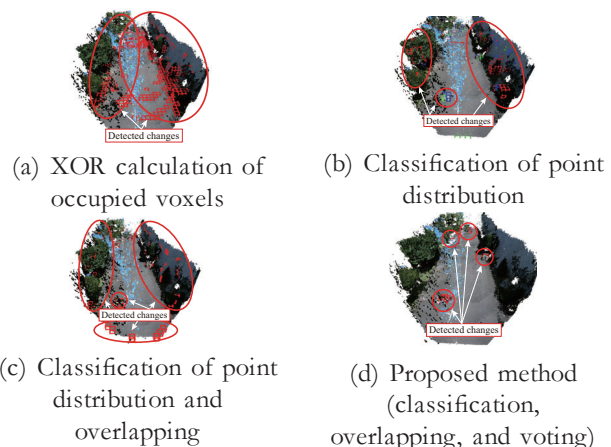


Fig. 8. Detected spatial changes (red, blue, and green cubes) in an outdoor environment.

VII. CONCLUSIONS

The present paper proposed a fast spatial change detection technique for a mobile robot using an on-board RGB-D/stereo camera and a high-precision 3D map created using a 3D laser scanner. This technique first converts point clouds in a map and measured data to grid data (ND voxels) using NDT and classifies the voxels into three categories. The voxels in the map and measured data are then compared according to the category and features of the ND voxels. The proposed technique consists of the following three techniques.

- 1) Classification of the point distribution
- 2) Overlapping of voxels in map data
- 3) Voting of spatial change detection through sequential measurements

We conducted experiments using a mobile robot equipped with real-time range sensors in order to confirm the performance of the proposed real-time localization and spatial change detection techniques in indoor and outdoor environments.

Future work includes performance evaluation of actual scenes, such as stations or market areas, and improvement of the performance by using other information, such as color or laser reflectance. In particular, laser reflectance, which is obtained as a side product of range measurement by a laser scanner, is measured stably independent of the lighting condition, even at night. Therefore, as additional information, evaluating the spatial change robustly is very useful.

ACKNOWLEDGMENT

This research is supported by JSPS KAKENHI Grant Number JP26249029.

REFERENCES

- [1] M. Hebel, M. Arens, and U. Stilla, ‘‘Change detection in urban areas by object-based analysis and on-the-fly comparison of multi-view data,’’ *ISPRS Journal of Photogrammetry and Remote Sensing*, vol. 86, pp. 52–64, 2013.

- [2] T. T. Vu, M. Matsuoka, and F. Yamazaki, "Lidar-based change detection of buildings in dense urban areas," in *IGARSS 2004. 2004 IEEE International Geoscience and Remote Sensing Symposium*, vol. 5, pp. 3413–3416 vol.5, Sept 2004.
- [3] R. Zeibak and S. Filin, "Change detection via terrestrial laser scanning," *International Archives of Photogrammetry and Remote Sensing*, vol. 36, no. 3, pp. 430–435, 2007.
- [4] D. Lague, N. Brodu, and J. Leroux, "Accurate 3d comparison of complex topography with terrestrial laser scanner: Application to the rangitikei canyon (n-z)," *ISPRS Journal of Photogrammetry and Remote Sensing*, vol. 82, pp. 10 – 26, 2013.
- [5] B. Thomas, C. Remco, W. Zachary, and R. William, "Visual analysis and semantic exploration of urban lidar change detection," *Computer Graphics Forum*, vol. 27, no. 3, pp. 903–910, 2008.
- [6] G. Palma, M. Sabbadin, M. Corsini, and P. Cignoni, "Enhanced visualization of detected 3d geometric differences," *Computer Graphics Forum*, vol. 37, pp. 159–171, 2 2018.
- [7] Y. Li, X. Fan, N. J. Mitra, D. Chamovitz, D. Cohen-Or, and B. Chen, "Analyzing growing plants from 4d point cloud data," *ACM Trans. Graph.*, vol. 32, pp. 157:1–157:10, Nov. 2013.
- [8] D. Filliat and J.-A. Meyer, "Map-based navigation in mobile robots:: I. a review of localization strategies," *Cognitive Systems Research*, vol. 4, no. 4, pp. 243 – 282, 2003.
- [9] S. Thrun, D. Fox, W. Burgard, and F. Dellaert, "Robust monte carlo localization for mobile robots," *Artificial Intelligence*, vol. 128, no. 1, pp. 99 – 141, 2001.
- [10] S. Thrun, W. Burgard, and D. Fox, *Probabilistic Robotics (Intelligent Robotics and Autonomous Agents)*. The MIT Press, 2005.
- [11] A. Nuchter, H. Surmann, K. Lingemann, J. Hertzberg, and S. Thrun, "6d slam with an application in autonomous mine mapping," in *Robotics and Automation, 2004. Proceedings. ICRA '04. 2004 IEEE International Conference on*, vol. 2, pp. 1998–2003 Vol.2, April 2004.
- [12] P. Biber and W. Strasser, "The normal distributions transform: a new approach to laser scan matching," in *Proceedings 2003 IEEE/RSJ International Conference on Intelligent Robots and Systems (IROS 2003) (Cat. No.03CH37453)*, vol. 3, pp. 2743–2748 vol.3, Oct 2003.
- [13] S. Oishi, Y. Jeong, R. Kurazume, Y. Iwashita, and T. Hasegawa, "Nd voxel localization using large-scale 3d environmental map and rgbd camera," in *2013 IEEE International Conference on Robotics and Biomimetics (ROBIO)*, pp. pp.538–545, 2013.
- [14] H. Andreasson, M. Magnusson, and A. Lilienthal, "Has something changed here? autonomous difference detection for security patrol robots," in *2007 IEEE/RSJ International Conference on Intelligent Robots and Systems*, pp. 3429–3435, Oct 2007.
- [15] P. Nüñez, P. Drews, A. Bandera, R. Rocha, M. Campos, and J. Dias, "Change detection in 3d environments based on gaussian mixture model and robust structural matching for autonomous robotic applications," in *2010 IEEE/RSJ International Conference on Intelligent Robots and Systems*, pp. 2633–2638, Oct 2010.
- [16] J. P. Underwood, D. Gillsjö, T. Bailey, and V. Vlaskine, "Explicit 3d change detection using ray-tracing in spherical coordinates," in *2013 IEEE International Conference on Robotics and Automation*, pp. 4735–4741, May 2013.
- [17] A. W. Vieira, P. L. J. Drews, and M. F. M. Campos, "Spatial density patterns for efficient change detection in 3d environment for autonomous surveillance robots," *IEEE Transactions on Automation Science and Engineering*, vol. 11, pp. 766–774, July 2014.
- [18] M. Fehr, F. Furrer, I. Dryanovski, J. Sturm, I. Gilitschenski, R. Siegwart, and C. Cadena, "TsdF-based change detection for consistent long-term dense reconstruction and dynamic object discovery," in *2017 IEEE International Conference on Robotics and Automation (ICRA)*, pp. 5237–5244, May 2017.
- [19] L. Luft, A. Schaefer, T. Schubert, and W. Burgard, "Detecting changes in the environment based on full posterior distributions over real-valued grid maps," *IEEE Robotics and Automation Letters*, vol. 3, pp. 1299–1305, April 2018.
- [20] P. Biber and W. Strasser, "The normal distributions transform: a new approach to laser scan matching," in *Proceedings 2003 IEEE/RSJ International Conference on Intelligent Robots and Systems (IROS 2003) (Cat. No.03CH37453)*, vol. 3, pp. 2743–2748 vol.3, Oct 2003.
- [21] J. P. Saarinen, H. Andreasson, T. Stoyanov, and A. J. Lilienthal, "3d normal distributions transform occupancy maps: An efficient representation for mapping in dynamic environments," *The International Journal of Robotics Research*, vol. 32, no. 14, pp. 1627–1644, 2013.
- [22] P. Gianpaolo, C. Paolo, B. Tamy, and S. Roberto, "Detection of geometric temporal changes in point clouds," *Computer Graphics Forum*, vol. 35, no. 6, pp. 33–45, 2016.
- [23] P. J. Besl and N. D. McKay, "A method for registration of 3-d shapes," *IEEE Transactions on Pattern Analysis and Machine Intelligence*, vol. 14, pp. 239–256, Feb 1992.
- [24] H. Murakami, K. Nakagawa, H. Hasegawa, T. Shibata, and E. Iwanami, "Change detection of buildings using an airborne laser scanner," *ISPRS Journal of Photogrammetry and Remote Sensing*, vol. 54, no. 2, pp. 148 – 152, 1999.
- [25] "Spatial change detection on unorganized point cloud data." http://pointclouds.org/documentation/tutorials/octree_change.php.
- [26] D. Girardeau-Montaut, M. Roux, R. Marc, and G. Thibault, "Change detection on points cloud data acquired with a ground laser scanner," *International Archives of Photogrammetry, Remote Sensing and Spatial Information Sciences*, vol. 36, no. PART 3, pp. 30–35, 2005.
- [27] T. Pollard and J. L. Mundy, "Change detection in a 3-d world," in *2007 IEEE Conference on Computer Vision and Pattern Recognition*, pp. 1–6, June 2007.
- [28] A. O. Ulusoy and J. L. Mundy, "Image-based 4-d reconstruction using 3-d change detection," in *Computer Vision – ECCV 2014* (D. Fleet, T. Pajdla, B. Schiele, and T. Tuytelaars, eds.), (Cham), pp. 31–45, Springer International Publishing, 2014.
- [29] M. Magnusson, H. Andreasson, A. Nuchter, and A. J. Lilienthal, "Appearance-based loop detection from 3d laser data using the normal distributions transform," in *2009 IEEE International Conference on Robotics and Automation*, pp. 23–28, May 2009.